

On the origin of multiple time scales in the relaxation of protein hydration layer: A molecular dynamics simulation study

Sayantan Mondal¹, Saumyak Mukherjee² and Biman Bagchi*

Solid State and Structural Chemistry Unit

Indian Institute of Science, Bangalore, India

E-mail: *profbiman@gmail.com

Abstract

In order to inquire the microscopic origin of observed disparate time scales of relaxation in protein hydration layer (PHL), we carry out several computer experiments using atomistic molecular dynamics simulations. We (i) mutate the charges of the AASC in the neighbourhood of certain natural probes (Tryptophan) in Lysozyme, Myoglobin and Monellin, and also (ii) freeze the side chain motions. In subsequent analyses, we decompose the total solvation energy response in terms of various contributions present in the system to capture the interplay among different self and cross-energy correlation terms. The main results are as follows. (1) We establish the existence of a significant slow component in the contribution from the water molecules present within the PHL. Both charged amino acid side chain (AASC) residues and the water molecules in the PHL contribute (water more than side chains) to the slow response measured. Generally speaking, AASCs contribute with time scales of ~100-300 ps while water contributes with shorter time scales, in ~30-100 ps range. Moreover, these motions are strongly coupled. Freezing protein motion removes the slowest component but a part remains due to water. In earlier studies, slowness that arises from PHL was missed because of a large contribution from the bulk water to solvation energy. (2) Thus, the separation in spatial and temporal response in solvation dynamics reveals different roles of PHL and bulk water. The PHL water molecules are largely responsible for the slow component whereas the initial ultrafast decay arise predominantly (~80%) from the water molecules in the bulk. This is in agreement with earlier theoretical observations. (3) The origin of the coupling between water molecules in the PHL and AASC can be attributed (at least partly) to the presence of charges in the AASC around a selected probe. The charge enforces a structural ordering of nearby water molecules and helps forming long-lived hydrogen bonded network. (4) Removal of the charges and protein motions allows a faster relaxation, although a slow component (~30-80 ps) (that is not present in the bulk) remains in solvation. This is the characteristic of slow water molecules inside PHL. We attempt to rationalise these facts with the help of a molecular hydrodynamic theory that was developed using classical time dependent density functional theory in a semi quantitative manner.

¹ E-mail: sayantan0510@gmail.com

² E-mail: mukherjee.saumyak50@gmail.com

*corresponding author

I. INTRODUCTION

Water molecules that surround a protein (or other biomolecules like DNA) play a major role in providing stability to the native structure. Biological activities of these biomolecules are also dependent on the dynamics of protein hydration layer (PHL).¹⁻¹⁸ Because of its immense importance in biology, PHL has remained a subject of substantial interest.^{15-17,19-29} With the help of various theoretical and experimental methodologies, new insights into the nature of PHL are emerging.^{30,31}

An estimation of the possible width of the PHL came from the elongated rotational time constants of water molecules measured by nuclear magnetic resonance (NMR) experiments in several aqueous proteins. This eventually directed to the concept of the ‘iceberg model’.^{32,33} Later, the landmark work of Wüthrich dispelled the idea of such a rigid layer of water molecules around a protein by calculating residence time of water inside PHL (found to be ~300 ps)^{29,34}. Even earlier than the reported NMR results, Pethig, Grant and others studied aqueous solutions of proteins using dielectric spectroscopy¹⁹. They found three discrete timescales ~10 ps, ~10 ns and ~40 ps (the delta-dispersion attributed to PHL) which were later verified by Mashimo^{21,35}.

Much later, this problem was revisited by Halle *et al.* using an improved NMR technique widely known as magnetic relaxation dispersion (MRD)^{27,36}. These studies suggested the absence of any substantially slow component in the dynamics of PHL. Halle *et al.* suggested that any relaxation process is slowed down maximum by a factor of ~2-4. This estimate seems to contradict the findings of both dielectric relaxation and of solvation dynamics. Several time dependent fluorescence Stokes shift (TDFSS) and computer simulation studies were carried out by Zewail, Bhattacharyya, Maroncelli, Fleming and others^{7,8,12,37-40}. All these studies reported observation of a component in the long time that was substantially slower than what was observed in the bulk.

Although NMR results tend to discard the existence of any slow component, MRD could successfully predict the width of the distribution of rotational time constants of individual water molecules. In a recent work, we duly addressed the origin and solution to this discrepancy³⁰. It was pointed out that while average might be slower by a

mere factor ~2-4, the distribution might look completely different with an order of magnitude slower dynamics at the late stage of relaxation (that is a log-normal distribution).

One aspect that is often ignored in the discussions of PHL dynamics is the sensitivity of the dynamics to different experimental probes. For example, NMR studies provide single particle dynamics but averaged over a large number of molecules³⁶. On the other hand dielectric relaxation derives contribution from all the molecules and hence a collective measure^{6,41}. Although there are a lot of efforts to describe the uniqueness of PHL as a whole, study of local structure and dynamics centred on a natural probe draws avid attention.

Apart from dielectric relaxation¹⁹⁻²¹ and NMR experiments^{26,36}, time dependent fluorescence Stokes shift^{7,11,42-44} (TDFSS) and three pulse photon echo peak shift (3PEPS)⁴⁵⁻⁴⁷ are used to study the local dynamics around a probe. More recently, Kubarych *et al.* have used 2D-IR spectroscopy to find out the orientational slowness of PHL⁴⁸. TDFSS experiments measures the time dependent frequency, $\nu(t)$, of a fluorescence probe in order to construct a non-equilibrium stokes shift response function (**Eq.[1]**).^{1,38,44,49-51}

$$S(t) = \frac{\nu(t) - \nu(\infty)}{\nu(0) - \nu(\infty)} = \frac{E_{solv}(t) - E_{solv}(\infty)}{E_{solv}(0) - E_{solv}(\infty)} \quad [1]$$

Where, $E_{solv}(t)$ is the time-dependent energy response as measured by the probe at time ‘ t ’ (**Eq.[2]**).

$$E_{solv}(t) = -\frac{1}{2} \int d\mathbf{r} \mathbf{E}_0(\mathbf{r}) \cdot \mathbf{P}(\mathbf{r}, t) \quad [2]$$

Here, $\mathbf{E}_0(\mathbf{r})$ is the position dependent bare electric field of the polar solute (Tryptophan, a natural probe in our case). $\mathbf{P}(\mathbf{r}, t)$ is the position and time dependent polarisation which is related to dielectric relaxation⁷.

In order to obtain a brief understanding of the timescales involved in solvation, it is relevant to quantify solvation timescales for simple probes. Solvation of an ion in a dipolar liquid is faster compared to dielectric relaxation. Whereas,

solvation time constant for a dipole (τ_L^d) is slightly higher than that of an ion (τ_L) (Eq.[3]).³⁷

$$\tau_L = \left(\frac{\epsilon_\infty}{\epsilon_0} \right) \tau_D$$

$$\tau_L^d = \left(\frac{2\epsilon_\infty + \epsilon_c}{2\epsilon_0 + \epsilon_c} \right) \tau_D$$

[3]

Here, τ_D is the Debye relaxation time; ϵ_c is the dielectric constant of the molecular cavity; ϵ_0 and ϵ_∞ are respectively the static and infinite frequency dielectric constants of the solvent. It is not straightforward to define an effective dielectric constant³¹ of a local region like the PHL because dielectric constant is inherently a collective quantity where cross-correlation between different molecules play quite an important role. Solvchromatic studies and simulations³¹ suggest that the effective dielectric constant inside the PHL is nearly half of that in bulk water. As result the solvation may slow down by nearly a factor of two. Note that, there can be other reasons for the slowness.

In neat water, in addition to an ultrafast component, there are two timescales of the order of $\sim 270\text{fs}$ and $\sim 1\text{-}2\text{ps}$ ^{45,51,52}. The complex solvation in the bulk gets even more complicated for hydration water. In addition to the multitude of timescales there is a dominant role of coupling between the motions of side-chain and water, which still deserves proper quantification. According to the “unified model for protein dynamics” proposed by Frauenfelder *et al.* there exists slaving of small scale and large scale protein motions by hydration and bulk water molecules respectively.^{5,53}

In a series of studies, Zewail *et al.* observed the presence of a slow component in solvation with the help of TDFSS of natural probe tryptophan using femtosecond lasers of limited resolution. That is, with their laser setup, they were unable to detect the ultrafast component but could successfully detect the slower components. Tryptophan in proteins like *Subtilisin Carlsberg* and *Monellin* typically shows a bimodal decay (one less than $\sim 1\text{ps}$ and another in $\sim 20\text{-}40\text{ ps}$ range).^{7,43} Recent experiments also suggest the presence of slow timescales ($\sim\text{ps}$ regime) but, along with an ultrafast component.⁵⁴ Bhattacharyya *et al.* obtained

timescales in the order of few hundred ps to a few ns.^{8,39,40} Fleming and co-workers used 3PEPS to study solvation of eosin dye tied to Lysozyme surface captured the presence of two distinct slow timescales ($\sim 100\text{ ps}$ and $\sim 500\text{ ps}$) that were absent for eosin in neat water⁴⁵. Zhong *et al.* employed site directed mutations on sperm whale myoglobin which led to a spectrum of relaxation timescales ($\sim 1\text{-}8\text{ ps}$ and $\sim 20\text{-}200\text{ ps}$)⁵⁵ that are present at different sites of the same protein. The same group has also studied the effect of charges on the timescales using alanine scan method at different sites.⁵⁶

In fact, the origin of slowness in the dynamics of protein hydration layer is still an unsettled issue. There could possibly be two distinct origins. First is protein conformation fluctuation and second is the slow water molecules hydrogen bonded to charge groups on the surface of a protein. The latter mechanism was proposed by Nandi and Bagchi some time ago as an explanation of slow time scale observed in the dielectric relaxation measurements.^{6,57} MD simulations reveal that freezing the protein motions results in a faster solvation at W7 site of apomyoglobin.⁴² In earlier studies, Zhong *et al.* and others showed the multitude and heterogeneity of solvation timescales at different sites of a same protein. It was stated that charged/polar residues as well as the side-chain fluctuations play a major role in slowing down the local dynamics.^{15,42,56} But, the role of water molecules inside the PHL in slowing down the dynamics and their relative contribution is not properly addressed.

The present study aims to unveil the microscopic details and establishes the origin of slow timescale in solvation dynamics. We attempt to resolve one of the long standing debates in this field. “*What are the prevailing factors responsible for the slow solvation in PHL: water, protein or a coupled motion?*” Also, why different experiments give such different results?

We choose several intrinsic natural tryptophan (W) probes in (i) Myoglobin (W7) (ii) Lysozyme (W123) and (iii) sweet protein Monellin (W3). Mutation of the neighbourhood of natural probes and decomposition of the solvation energy into various components reveal information on how they can affect the local structure and dynamics. This work provides a logical and semi-quantitative

explanation of the timescales of solvation dynamics at different sites of the protein and also the reason for their existence.

An important aspect that is often overlooked is the spatial dependence of the temporal response. Both TDFSS and dielectric relaxation experiments measure response which is sum of the response from water molecules in the first layer and the outer layer. A molecular hydrodynamic theory predicts dynamic response to depend on the length scale of the process. Thus, first layer response is predicted to be slower than that of the bulk. Our results are consistent with this prediction.

The organisation of the rest of the paper is as follows: In the next section (**Section II**), we discuss the details of computer experiments. In **Section III**, we report and explain the results obtained by analysing the MD trajectories. This section is divided into several sub-sections. In subsequent sections (**Section IV** and **V**) we rationalise the obtained numerical data with the help of a time dependent density functional theory (TDDFT) based molecular hydrodynamic theory (MHT) description. In **Section VI**, we end with the importance of these findings on solvation dynamics, and also with some general conclusions.

II. COMPUTER EXPERIMENTS AND METHODS OF ANALYSES

In order to profoundly establish the origin of the slow as well as the ultrafast component in solvation of natural probes, we perform the following two kinds of computer experiments- (a) Mutation of the neighbourhood AASCs (within ~ 7 - 8\AA of the probe) of a certain natural probe and (b) Freezing the AASC residues (that is, the whole protein's natural motions are quenched). The first set of experiments allows us to investigate the role of charges in the surroundings of a natural probe on solvation dynamics. Whereas, the second set of experiments allows us to remove the effect of the inherent AASC fluctuations. So there can be following four such scenarios. (i) A non-zero net charge around the probe and protein is mobile, (ii) No net charge around the probe but protein is mobile, (iii) There is a net charge around the probe but protein is frozen and (iv) No net charge around the probe and the protein is also frozen. The natural surroundings (wild type) of the chosen probes are noted down in **Table 1**. The information on mutation is provided in the *Supporting Information* section.

Table 1. Surroundings of the selected natural probe tryptophan in Lysozyme, Myoglobin and Monellin.

Probe	Protein	Residues in the neighbourhood	Surroundings (wild type)	Surroundings (mutant)
W7	Myoglobin	E4, E6, K77, K78, K79, K133	Charged	Charges removed
W123	Lysozyme	R5, K33, R114, K116, D119, R125	Charged	Charges removed
W3	Monellin	E2, E4, K44, E59, D74	Charged	Charges removed

We mutate to neutralise the charges of the neighbourhood residues of tryptophan (see *Supporting Information S1* for details). Solvation time correlation functions (TCFs) are then

calculated for wild type and mutated proteins. Furthermore, we perform simulations by quenching the protein motions and calculate solvation TCFs.

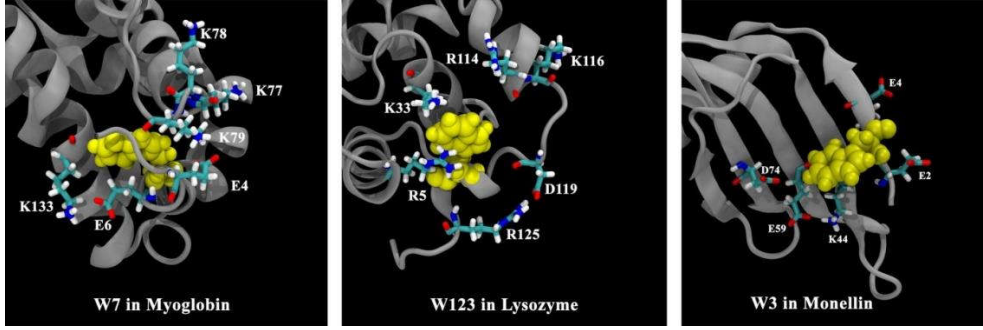


Figure 1. Snapshots from MD simulations ($t=0$) showing the neighbourhood of natural probes, W7 in Myoglobin (left), W123 in Lysozyme (middle) and W3 in sweet protein Monellin (right). Tryptophan residues (used as a natural probe) are shown in yellow.

First, we observe the local structural ordering of water molecules around a natural probe with/without the presence of neighbourhood charges. Proper quantification arises in the form of radial distribution function (RDF) between relevant side-chain atoms and water.

On the other hand, TDFSS experiments can provide time dependent fluorescence frequency, $\nu(t)$ (Eq.[1]) for a probe. Though $S(t)$ is a non-equilibrium response function, under the assumption of linear response theory⁵⁸, we can calculate $S(t)$ from the equilibrium energy time correlation function $C(t)$ (Eq.[4]).^{38,50,51,59-61}

$$C(t) = \frac{\langle \delta E_{solv}(0) \delta E_{solv}(t) \rangle_{gr}}{\langle \delta E_{solv}(0) \rangle^2_{gr}} \quad [4]$$

Here, $\delta E_{solv}(t)$ is the fluctuation given by; $\delta E_{solv}(t) = E_{solv}(t) - \langle E \rangle_{gr}$. The subscript ‘gr’ indicates averaging over ground state only.

For further analysis, we decompose the time dependent solvation energy $E_{solv}(t)$ into the components present in the system, namely $E_{sc}(t)$, $E_{core}(t)$, $E_{wat}(t)$ and $E_{ion}(t)$ as depicted in Eq.[5]^{61,62}. Pal *et al.*, as a first, used this decomposition method.⁶²

$$E_{solv}(t) = E_{sc}(t) + E_{core}(t) + E_{wat}(t) + E_{ion}(t) \quad [5]$$

We find contributions from terms involving ions are negligible compared to others. Hence, we can express total solvation time correlation function as a summation of three self and six cross-correlation terms (Eq.[6]).

$$S(t) = \sum_{\alpha} S_{\alpha\alpha}(t) + \sum_{\alpha} \sum_{\beta} S_{\alpha\beta}(t) \quad [6]$$

Where, α and β stand for different components. The normalised total solvation energy correlation plots are fitted to a multi-exponential form along with a Gaussian component (τ_g) which provides information regarding the ultrafast dynamics as given by Eq.[7].

$$S(t) = a_g e^{-\left(\frac{t}{\tau_g}\right)^2} + \sum_{i=1}^n a_i e^{-\left(\frac{t}{\tau_i}\right)}; n=2 \quad [7]$$

τ_1 and τ_2 are another two timescales (intermediate and slow relaxation). It is justifiable on the ground that the ultrafast component is noticeably faster than the exponential ones and it carries $\sim 100\%$ weightage at $t=0$. The average time constants ($\langle \tau \rangle$) are calculated by integrating $S(t)$ with respect to time⁴⁴.

In order to precisely identify the governing factor in slow and ultrafast part of dipolar solvation dynamics we further dissect the water contribution into two parts- (i) contribution arising due to water molecules inside $\sim 1\text{nm}$ which characterise PHL and (ii) contribution arising due to the water molecules in the outer layer.

III. RESULTS AND DISCUSSIONS:

A. Enhancement of local structure of water in the presence of charges

We calculate the pair correlation function (i.e., RDF) between the N_{ε} of indole moiety of the natural probe and oxygen atoms of water molecules in order to investigate the local structural changes of water in presence/absence of neighbourhood

charges. For W123 in Lysozyme, an extra peak around $\sim 4.7\text{\AA}$ is present while there are charges nearby in the wild type lysozyme (Figure 2a). Similarly for W7 in Myoglobin, an enhancement of the first and second peak height is observed while the probe is surrounded by charges (Figure 2b). However, in case of W3 in Monellin, the wild type

and the mutant shows almost similar $g(r)$ plots. This is mainly because W3 in Monellin is sufficiently exposed to water in both wild and mutant type. Nevertheless, structural enhancement, though not much, can be noticed and the presence of the third small peak while surrounded by charges suggests long range ordering.

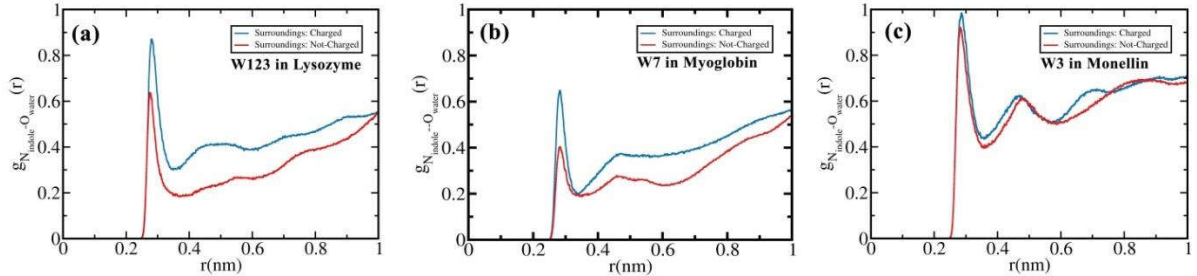


Figure 2. Radial distribution functions (RDF) for indole-nitrogen (of natural probe tryptophan) and water-oxygen pair. (a) RDF for W123 in Lysozyme; Wild type (blue) and neighbourhood mutated W123 (red). (b) RDF for W7 in Myoglobin; Wild type (blue) and neighbourhood mutated W7 (red). (c) RDF for W3 in sweet protein Monellin; Wild type (blue) and neighbourhood mutated W3 (red). [The colour codes are maintained such that blue represents charged environment whereas red represents neutral environment.]

It is clear from Figure 2 that the distortion of the water structure and certain rigidity that is not present in bulk water. These are the result of strong electrostatic interaction and long lived hydrogen bonds between the charges and the water molecules. Lowering of the peak height is also suggestive of the fact that a less number of water molecules are in the vicinity of the probe. This indeed affects the solvation timescales which we discuss in the subsequent sections.

B. Solvation Dynamics of Tryptophan: Effect of charges and side-chain fluctuations

Solvation energy relaxation of natural probe tryptophan inside PHL shows ubiquitous bimodal nature along with a sub 100fs ultrafast inertial component. However, it has been missed by many TDFSS experiments because of compromising resolution of the laser. W7 in the mutant myoglobin, where charged residues in the vicinity are made neutral, average solvation relaxation becomes faster by a factor of 2.5. Both the value and amplitude of the slowest timescale reduces (Table 2). On the other hand, W123 in mutated lysozyme also shows a faster relaxation when the charges are mutated to provide a neutral surroundings. The average solvation time constant also gets slightly reduced on removal of the charges (Table 2). However, the slow timescale are comparable (~ 120 - 130 ps) in both the cases. Surprisingly, W3 in monellin shows some

anomaly. Because of the removal of charges, the initial decay was faster than that of the wild type as expected. At longer times (after 20 ps), the slowest timescale becomes larger although possesses a smaller amplitude. Average timescales are however comparable. The reason of the anomaly may be speculated in terms of the location and immediate surroundings of the probe. Each protein that is selected for our study falls in different classes (See **Supporting Information S2** for details). However, further detailed study is required to profoundly establish the sensitivity of dynamics to the site specificity of the protein.

Upon freezing the motion of the protein (wild type) we can separate out the timescales that may arise solely because of the combined effect of water in the PHL and bulk. Solvation becomes faster. The slowest component above ~ 100 ps disappears when the AASC atoms are not fluctuating. This indicates the role of AASC fluctuations in slowing down the solvation substantially. But a slow component within ~ 20 - 90 ps is still present which is indeed a lot slower than bulk. In case of W7 in myoglobin it is 84.9 ps (18%); for W123 of lysozyme it is 38.3 ps (7%) and for W3 in monellin it takes up a value of 23.5 ps (4%). We attribute this to the slow orientational and translational motion of water inside PHL³⁰. We establish this fact in Sec III.C. Note that the trend (i.e. upon removal of charges/fluctuations) of the

relaxation behaviour is not same for these three probes. Different sites responses differently that too

varies from protein to protein.

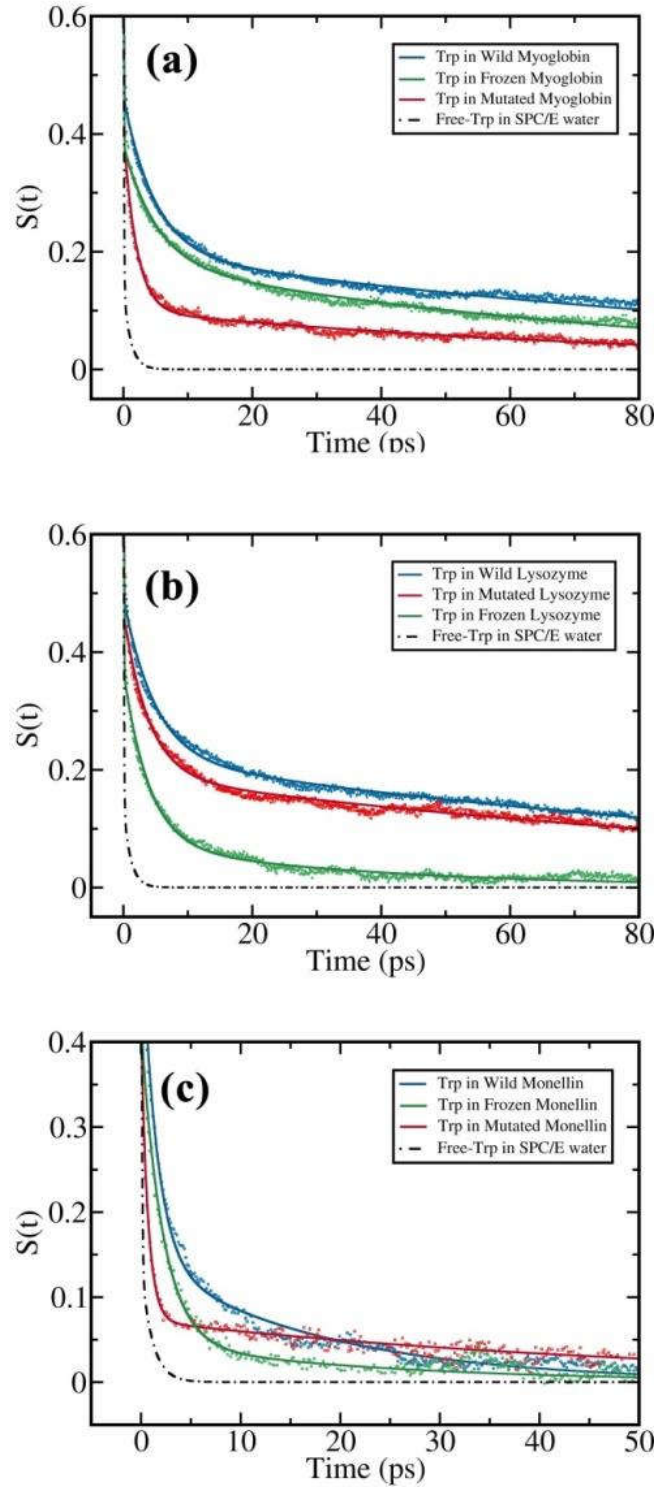


Figure 3. Normalised total solvation energy time correlation function (TCF) for natural probes in Lysozyme, Myoglobin and Monellin. TCFs of probe with surrounding charges are shown in blue, without surrounding charges are shown in red and that of frozen conformations are shown in green. (a) W7 in myoglobin, (b) W123 in lysozyme and (c) W3 in monellin. Solvation energy relaxation for free tryptophan in SPC/E water is extremely fast as compared to that of protein surfaces (shown in black). [Initial ultrafast decay is ubiquitous and hence omitted from the plots.]

Table2. Timescales (parameters after fitting to Eq.[7]) of solvation energy relaxation for two natural probes in Myoglobin, Lysozyme and Monellin, along with a free tryptophan in SPC/E water.

Probe	Protein	Surroundings	a_g	$\tau_g (ps)$	a_1	$\tau_1 (ps)$	a_2	$\tau_2 (ps)$	$\langle \tau \rangle (ps)$
W7	Myoglobin (Mgb)	<i>Wild Type, Charged</i>	0.54	0.092	0.26	4.80	0.20	120.6	25.0
		<i>Mutated, Charge removed</i>	0.59	0.082	0.31	1.99	0.10	92.2	9.8
		<i>Wild type, Frozen</i>	0.62	0.071	0.20	5.05	0.18	84.9	16.3
W123	Lysozyme (Lyso)	<i>Wild Type, Charged</i>	0.51	0.094	0.27	4.83	0.22	130.4	29.9
		<i>Mutated, Charge removed</i>	0.53	0.087	0.28	3.88	0.19	121.5	24.2
		<i>Wild type, Frozen</i>	0.63	0.090	0.30	3.91	0.07	38.3	3.9
W3	Monellin (Mon)	<i>Wild Type, Charged</i>	0.44	0.061	0.41	1.50	0.15	18.2	3.2
		<i>Mutated, Charge removed</i>	0.59	0.037	0.34	0.69	0.07	52.3	3.9
		<i>Wild type, Frozen</i>	0.56	0.07	0.37	2.13	0.04	23.5	1.8
Free-Trp	---	---	0.84	0.07	0.16	1.1	---	---	0.23

The above data indicate that the nearby charges play a major role in slowing down local dynamical responses. It is, again, primarily because of the long-lived hydrogen bonds those residues can form with surrounding water molecules which cannot orient rapidly (Sec 3.5).

C. Decomposition of solvation energy into self and cross correlation terms

According to Eq.[5], we decompose solvation response measured by the natural probes into several partial terms. Based on that, we calculate partial energy correlation functions for W123 and W7 in wild and mutant protein. There are some common features. Solvation of both the probes (Figure 4a) draws most of its contribution from Wat-Wat self-term. As these probes are fairly exposed,

water contribution is expectedly predominant. Nevertheless, the SC-SC/Core-Core self-terms also adds a considerable slow component. Few cross terms are anti-correlated which indicates that increased contribution from one component results in a decrease of the other one. The negative amplitude of such cross also helps in a faster relaxation and in dilution of slow timescales.

In the case of W123; both SC-SC and Wat-Wat terms show substantial slow decays (Figure 4). Core-Core self-term and Core-Wat cross terms are negligible. SC-Wat terms become anti-correlated and neutralise the huge slowness as well as amplitude arising from SC-SC and Wat-Wat terms. The faster decay for the mutant lysozyme is because of the presence of large amplitude slowly decaying anti-correlated SC-Wat cross terms, as compared to wild type. (Figure 4)

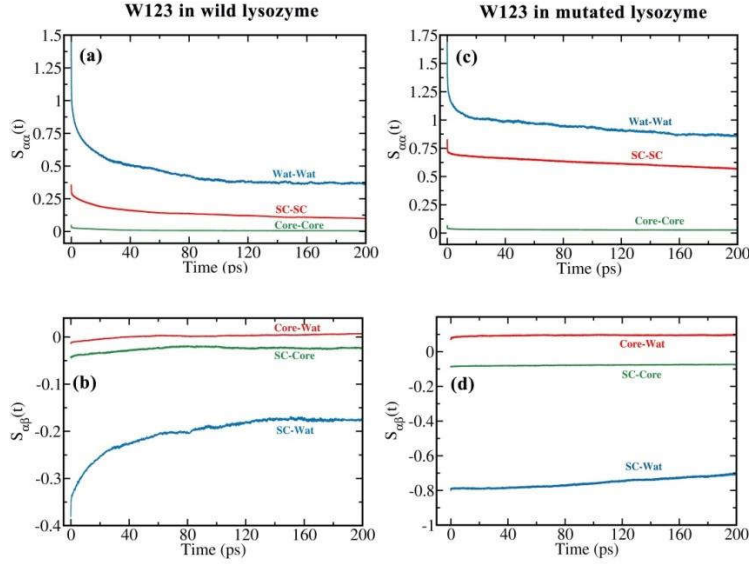


Figure 4. Partial self and cross energy correlation terms, relative to the amplitude of total energy correlation, for tryptophan-123 in wild type and its neighbourhood mutated protein. (a) self-terms in wild-type lysozyme. (b) cross-terms in wild-type lysozyme. (c) self-terms in mutated lysozyme. (d) cross-terms in mutated lysozyme.

On the other hand, in the case of W7, in both wild and mutated myoglobin, interaction with protein backbone (core) plays an important role. When surrounded by charged side-chains, the SC-SC term has an amplitude ~ 0.2 that drops to nearly

zero for the mutated protein. However in the wild type, SC-Wat terms are not anti-correlated (Figure 5). But, here as well, the water self-term plays a major role in the overall relaxation.

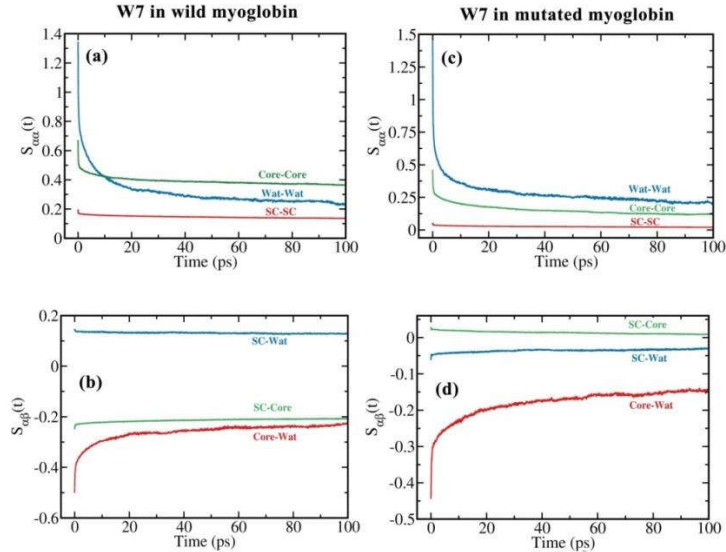


Figure 5. Partial self and cross energy correlation terms, relative to the amplitude of total energy correlation, for tryptophan-7 in wild type and its neighbourhood mutated myoglobin. (a) self-terms in wild-type. (b) cross-terms in wild-type. (c) self-terms in mutant. (d) cross-terms in mutant.

The partial correlation terms could explain Figure 3. Freezing results in a very fast decay for W123 but not so much for W7. This is because the neighbours (which contribute the most to the SC terms) of W123 are branched (a lot of arginines) as compared to that of W7 (glutamates and lysines). As a result, the solvation energy relaxation becomes

strongly dependent on the side-chain fluctuations in case of W123, but not to that extent in case of W7.

As it is clear from Figure 4 and Figure 5, that water plays a significant role in the overall solvation. The initial ultrafast decay is a contribution from water molecules in the outer

layer. To look into the water term more closely we further separate the contribution from PHL and outer layer. We find that $\sim 80\%$ of the ultrafast part (sub ~ 100 fs) is mainly due to the outer layer. In fact, outer layer make no contribution to the slowly decaying part.

Therefore the slow solvation energy relaxation is a combined contribution from PHL and AASC. When the protein is mobile, the water molecules in PHL can alone contribute $\sim 20\text{-}30\%$ to the slow time component in the $\sim 200\text{ps}$ timescale that gets diluted in the presence of several anti-

correlated cross terms. We find by freezing the protein that time constant of the slow decay remains $\sim 120\text{ps}$ that contributes $\sim 10\%$. When we do the mutation by removing the surrounding charges, we find a small increase in the rate. The absence of charges affects the slow component in PHL as the H-bond network is destroyed (see Sec III.E). The extra slowness arising from PHL in case of mobile protein is because of the presence of AASC motions that are coupled to the motion of water molecules inside PHL. Figure 6 shows an exemplary plot for W7 of myoglobin.

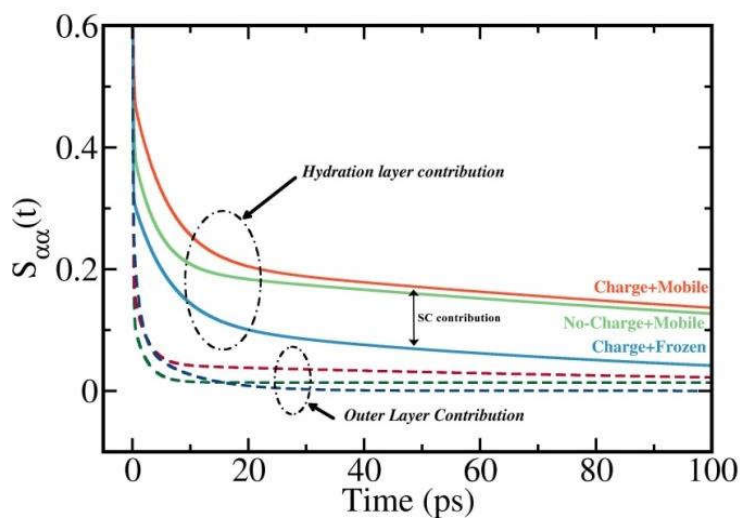


Figure 6. Normalised partial solvation time correlation functions that dissect the total water self-term into contributions from hydration layer and outer layer for W7 in myoglobin. Solid lines represent the contributions from PHL and dotted lines correspond to bulk counterparts. (Colour codes are maintained such a way that the darker shades of the same colour represent the bulk contribution)

This indicates that *the PHL water molecules can slow down solvation but not to that extent without the protein motions. This depicts the dynamically coupled motion between protein and hydration layer.*

D. Solvation of probes in frozen proteins: Contribution from water

To separate out the contribution arising solely from water, the protein motions are frozen.

So that, the self and cross terms involving SC and Core goes to zero. We are only left with water contribution. Of course, as discussed earlier, freezing results in a faster decay due to the absence of two slow sources. These are (i) AASC motions and (ii) dynamical coupling between AASC and PHL. Still we find a slow component below 100 ps for every probe in charged/uncharged surroundings. There can be no other sources other than the slow water molecules in the PHL itself.

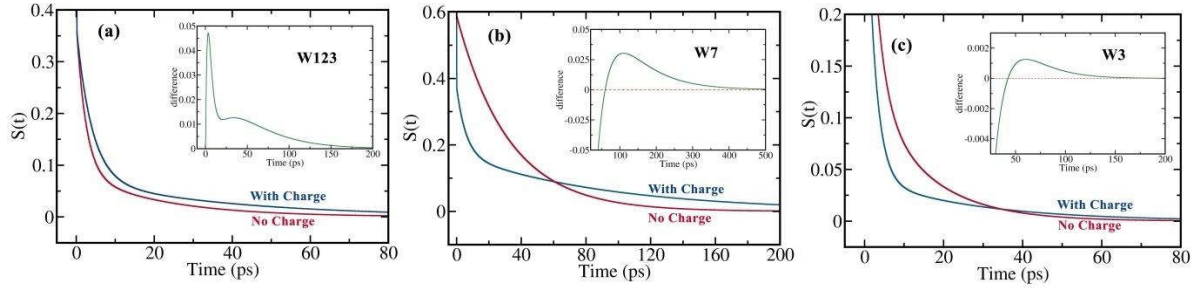


Figure 7. Comparisons of normalised total solvation time correlation functions (TCF) for tryptophan in frozen protein in case of polar/non-polar environment. (a) Normalised TCF for W123 in frozen lysozymes. (b) Normalised TCF for W7 in frozen myoglobin. (c) Normalised TCF for W3 in frozen monellin. In the insets, the difference plot is shown to point out the relative change in the nature of these plots with/without charged surroundings.

Table 3. Multi-exponential fitting parameters for the normalised solvation time correlation functions in case of frozen lysozyme (plots shown in Figure 7). The slow timescales even in the absence of side-chain motions are highlighted using boldfaces.

Probe	Type	Surroundings	a_g	$\tau_g (ps)$	a_1	$\tau_1 (ps)$	a_2	$\tau_2 (ps)$	$\langle \tau \rangle (ps)$
W7 (Mgb)	Wild	Charged	0.61	0.070	0.20	5.05	0.18	84.9	16.3
	Mutated	Not Charge	0.42	0.068	0.02	2.99	0.56	32.5	18.3
W123 (Lys)	Wild	Charged	0.63	0.090	0.30	3.91	0.07	38.3	3.9
	Mutated	Not Charged	0.62	0.067	0.29	2.44	0.09	21.3	1.9
W3 (Mon)	Wild	Charged	0.56	0.070	0.37	2.13	0.04	23.5	1.8
	Mutated	Not Charge	0.53	0.090	0.35	2.56	0.12	15.9	2.8

E. Hydrogen bond dynamics around W123 in lysozyme

In order to find out any possible connection between the local H-bond dynamics and solvation timescales, we study hydrogen bond population as well as lifetime studies between acidic hydrogens (H atoms connected to N-atoms of R5, R114, R125, K33 and K116) surrounding W123 and water molecules. The geometrical criteria (angle and distance) are used as discussed by Chandler *et. al.*⁶³ to define H-bonds between two pairs. The H-bond lifetime is investigated using two types of

correlation functions which is constructed using Heaviside step function formalism- (i) the intermittent H-bond correlation function ($\langle h(0)h(t) \rangle / \langle h(0) \rangle$) and (ii) Continuous H-bond time correlation function ($\langle h(0)H(t) \rangle / \langle h(0) \rangle$)^{64,65}. Here $h(t)$ adopts a value of '1' if the bond exists and '0' otherwise. On the contrary $H(t)$ becomes continuously '0' if the bond breaks for once.

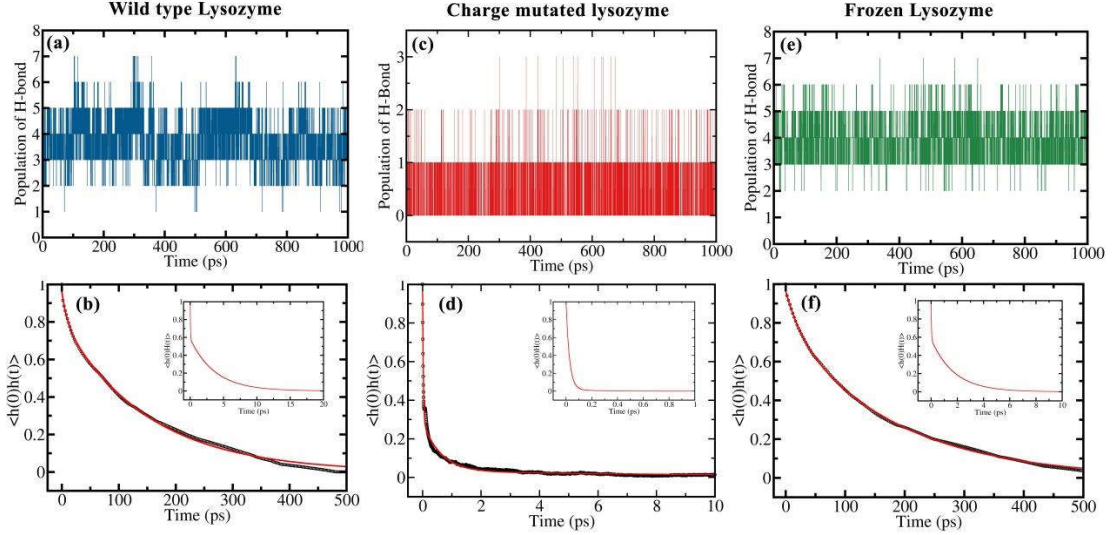


Figure 8. Plots representing the population and hydrogen bond lifetimes around W123 of Lysozyme. (a), (c) and (e) represent the population of H-bond between the surrounding charged residues and water molecules. (b), (d) and (f) correspond to the relaxation of intermittent H-bond time correlation function. The continuous H-bond time correlations are given in the insets.

We observe that lowering the charges, to make the surrounding AASCs neutral as a whole, destroys the H-bond network between AASCs and water to a huge extent (Figure 8). However, freezing doesn't affect the time constants for intermittent H-bond function to that extent, but it lowers the

timescales of continuous H-bond TCF. The latter is more informative on the lifetime of H-bonds. It also becomes clear from this study that long lived H-bond network is one of the governing factors of slow solvation.

Table 4. Multi-exponential fitting parameters for intermittent and continuous H-bond time correlation functions that are constructed using Heaviside step function.

Probe	Correlation function	Surroundings	a_1	$\tau_1 (ps)$	a_2	$\tau_2 (ps)$	a_3	$\tau_3 (ps)$	$\langle \tau \rangle (ps)$
W123	$\frac{\langle h(0)h(t) \rangle}{\langle h(0) \rangle}$	Wild Type, Charged	0.04	0.05	0.15	9.12	0.81	149.9	122.8
		Mutated, Charge removed	0.71	0.03	0.26	0.61	0.03	12.5	0.55
		Wild type, Frozen	0.03	0.09	0.18	26.7	0.79	181.1	147.8
W123	$\frac{\langle h(0)H(t) \rangle}{\langle h(0) \rangle}$	Wild Type, Charged	0.42	0.04	0.58	3.71	---	---	2.17
		Mutated, Charge removed	0.97	0.03	0.03	0.19	---	---	0.03
		Wild type, Frozen	0.34	0.03	0.66	1.75	---	---	1.2

IV. ORIGIN OF BOTH SLOW AND ULTRAFAST SOLVATION

It has been observed earlier that there is a ~60-70% sub 100 fs ultrafast component in the solvation of natural probes in water. This presence is ubiquitous. In our analysis as we have divided the response arising from water into PHL and outer layer responses, we have found that a significant contribution to the ultrafast component also arise from bulk part (Figure 6). This fact can be rationalised by a TDDFT based molecular hydrodynamic theory description developed by

Chandra and Bagchi^{49,66,67} back in the 1980s. The ultrafast dynamical components (libration, h-bond excitations and single particle rotation) of a dipolar liquid couple to the solvent polarisation to give rise to ultrafast solvation. We can write the expression of free-energy, assuming harmonic approximation, for polarisation fluctuation as in Eq.[8].

$$F(\{P_L(q)\}) = \frac{(2\pi)^3}{2V} \int dq K_L(q) P_L^2(q) \quad [8]$$

Here, $P_L(q)$ corresponds to the longitudinal component of polarisation fluctuation and $K_L(q)$ represents the wavenumber dependent force constant of $P_L(q)$. V is the volume. We can further write $K_L(q)$ in terms of wave number dependent dielectric function of the dipolar medium as Eq.[9].

$$K_L(q) = \frac{2}{(2\pi)^2} \frac{\varepsilon_L(q)}{\varepsilon_L(q) - 1} \quad [9]$$

$\varepsilon_L(q)$ assumes a large value at $q \rightarrow 0$ limit. Hence, $K_L(q)$ converges to $\frac{2}{(2\pi)^2}$. At large q , $\varepsilon_L(q)$ becomes unity and $K_L(q)$ diverges. Solvation energy doesn't derive much contribution from large q limit. Hynes *et. al.*^{68,69} earlier showed, with respect to the solvation of an ion, that the energy relaxation can be modelled as a relaxation in a harmonic polarisation potential. The curvature of such a well can be determined by $K_L(q)$. At small wavenumbers $K_L(q)$ is large and curvature is steep, hence it results in a faster relaxation.⁴⁴ The ultrafast component is essentially a long wavelength ($q=0$) phenomena which is probed by the bulk solvent. Whereas, the same theory predicts

$$\delta E_{solv}(\mathbf{r}, \Omega, t) = - \int d\mathbf{r}' d\Omega' C(\mathbf{r} - \mathbf{r}', \Omega, \Omega') \delta \rho(\mathbf{r}', \Omega', t). \quad [10]$$

Here, the primed variables are for the surrounding dipoles around a dipolar probe. This leads to the solvation time correlation function as the following,

$$\langle \delta E_{solv}(0) \delta E_{solv}(t) \rangle = \frac{1}{4\pi V} \int d\mathbf{r} d\Omega \langle \delta E_{solv}(\mathbf{r}, \Omega, 0) \delta E_{solv}(\mathbf{r}, \Omega, t) \rangle, \quad [11]$$

Where, V is the total volume of the system in which a free probe can reside in. But in our case the natural probes are bound to the protein that only allows a partial volume element to be considered. Now we

$$\begin{aligned} \delta E_{solv}(\mathbf{r}, \Omega, t) = & - \int d\mathbf{r}' d\Omega' C_{p-s}(\mathbf{r} - \mathbf{r}', \Omega, \Omega') \delta \rho_s(\mathbf{r}', \Omega', t) \\ & - \int d\mathbf{r}' d\Omega' C_{p-sc}(\mathbf{r} - \mathbf{r}', \Omega, \Omega') \delta \rho_{sc}(\mathbf{r}', \Omega', t) \end{aligned} \quad [12]$$

Here, 'p', 'sc' and 's' stand for probe, side-chain and solvent respectively. For further simplicity, we assume that the probe bound to the biomolecule as well as the surrounding AASC atoms are discrete

relaxation is slow at large wavenumbers (smaller distances) which is probed by the PHL.

V. TIME DEPENDENT DENSITY FUNCTIONAL THEORY ANALYSIS

In order to achieve a quantitative understanding of the important roles played by several self and cross energy correlation terms in the protein hydration layer dynamics, particularly those between AASC and water, we need a microscopic theoretical formulation. The only phenomenological theory at hand is the Nandi-Bagchi^{6,57} theory but that cannot explicitly describe the different terms involved. Such a microscopic formulation could be hard to achieve given the complexity of the system involved. Here we follow the previous works of Chandra and Bagchi^{41,67} and find that time dependent density functional theory can capture many of the interesting aspects at a semi-quantitative level.

Solvation energy measured by a probe (as given by Eq.[2]) is a function of position (\mathbf{r}), orientation (Ω) and time dependent polarisation which itself is expressed in terms of position, orientation and time dependent density field ($\delta \rho(\mathbf{r}, t)$) at that position.

$$\delta E_{solv}(\mathbf{r}, \Omega, t) = - \int d\mathbf{r}' d\Omega' C(\mathbf{r} - \mathbf{r}', \Omega, \Omega') \delta \rho(\mathbf{r}', \Omega', t). \quad [10]$$

break the integral in Eq.[11] into two terms with respect to two major contributions arising due to (i) AASC atoms and (ii) surrounding water molecules. This gives rise to Eq.[12].

charges instead of dipoles. So, we can drop the orientation dependence of side-chain and probe and rewrite Eq.[12] as,

$$\delta E_{solv}(r, t) = - \int dr' d\Omega' C_{p-s}(r - r', \Omega') \delta \rho_s(r', \Omega', t) - \int dr' C_{p-sc}(r - r') \delta \rho_{sc}(r', t) \quad [13]$$

Now, we fix the intermolecular frame along $(r - r')$ as z-axis and convert the integrals into integrals in Fourier space in order to apply density functional theory on solvation energy.

For further progress, the first term on the right hand side of **Eq. [13]** requires expansion of the direct correlation function and the density fluctuation term in terms of spherical harmonics, as

$$\begin{aligned} \langle \delta E_{solv}(0) \delta E_{solv}(t) \rangle = & \frac{1}{(2\pi)^3} \left[\int d\mathbf{k} C_{p-s}^2(\mathbf{k}) S_s(\mathbf{k}, t) \right. \\ & + \int d\mathbf{k} C_{p-sc}^2(\mathbf{k}) S_{sc}(\mathbf{k}, t) \\ & \left. + \int d\mathbf{k} C_{p-s}(\mathbf{k}) C_{p-sc}(\mathbf{k}) \langle \delta \rho_s(-\mathbf{k}, 0) \delta \rho_{sc}(\mathbf{k}, t) \rangle \right] \end{aligned} \quad [14]$$

First two terms are self-terms and the third one corresponds to the cross term. It is clear that the first two has no dependency on the sign of the direct correlation function $C(\mathbf{k})$ as they come in squares. But the third term carries a cross multiplication and its sign of the product becomes important, which is negative in some of our cases (**Figure 4**).

Furthermore, the dynamic structure factor ($S_s(\mathbf{k}, t)$) of solvent decays fast in the long wave number limit, and hence responsible for the fast decaying component similar to that of ion-solvation in bulk liquid. On the other hand, the $S_{sc}(\mathbf{k}, t)$ term is decay slowly and results in the slow components in the decay. The partial structure factor in the third term i.e. $\langle \delta \rho_s(-\mathbf{k}, 0) \delta \rho_{sc}(\mathbf{k}, t) \rangle$ may be either slow or fast depending on the location of the probe. Therefore, by freezing the protein motions we remove the slow contribution completely. This is the reason for the accelerated dynamics is observed and also reported by Singer *et al.*^{12,42}

VI. CONCLUSIONS

Solvation dynamics of natural probes in aqueous protein systems show a biphasic

explained in the molecular hydrodynamic theory. In the following we suppress the sum over (l, m) coefficients, for simplicity. We evaluate the energy time correlation function (**Eq.[13]**). This treatment gives rise to three terms in the solvation time correlation function, two self and one cross term. Hence, the expression becomes the following,

distribution of the dynamics along with a bulk like ultrafast component^{7,11,12,70,71}. The molecular mechanism behind the slow relaxation process near protein hydration layer, for example, the long components in TDFSS experiments, has been analysed in great detail by several groups.^{7-9,39,43} It was proposed that the slowness is due to the presence of ‘*biological water*’. Singer *et al.* contested this view and proposed instead of that the dynamical coupling between protein-water fluctuations is responsible for the slow timescale of solvation.⁴²

We have attempted to identify the causes of slow solvation inside PHL by employing several computer experiments. Here, we have shown that the charged side-chain residues indeed play an important role in slowing down the solvation. The presence of charges also facilitates long-lived H-bonds and local structural rigidity of water molecules. The energy decomposition technique, allows us to isolate the slow timescales that arises from the slow dynamics of PHL and AASC motions. Below we have provided a diagram, in the form of a flowchart, to elaborate the values and the sources of these timescales arising solely due to the water contribution, as observed in this study.

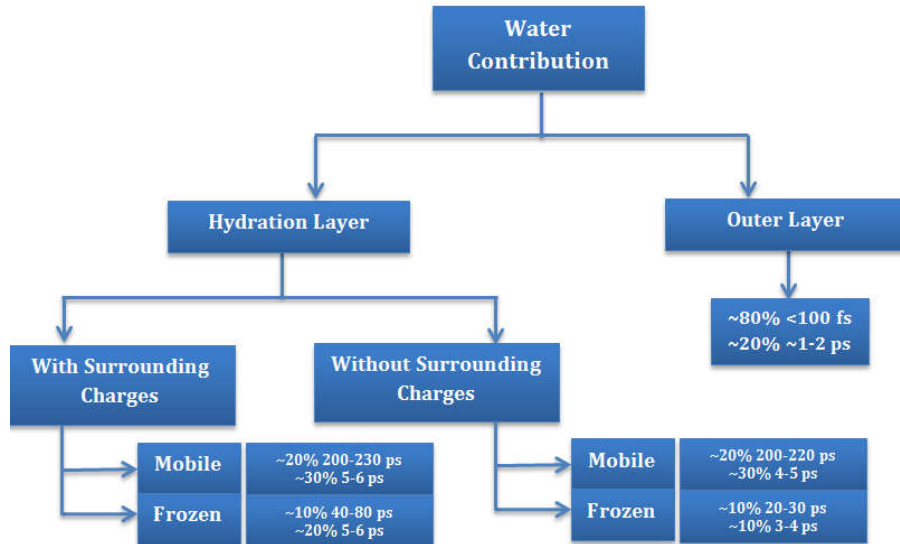


Figure 9. A schematic representation of the various sources of slow and ultrafast solvation along with their values, arising from protein hydration layer in solvation of a natural probe. Contribution from each part is individually normalised in calculating the % contributions.

We also observe the presence of dynamical coupling between AASC motions and water. *The slow component above or around 100 ps can only survive if the AASC motions are present, irrespective of charged/uncharged surroundings.* Timescales of solvation for frozen protein simulation typically produces timescales in the range of ~20-80 ps. On the other hand, the bulk solvent probes long wavelength modes and primarily responsible for the large amplitude of the sub-100 fs ultrafast solvation.

Another important factor often overlooked is that only the slow part of the total solvation energy is dominated by the water molecules in the protein hydration layer. It is the water in the PHL that is mostly responsible the intermediate time slower decay (with time constant in the ~30-40 ps range) along with some contribution from side-chain fluctuations. *We stress that this contribution slows down from sub ~1 ps in neat liquid to about ~40 ps when residing inside PHL.* The amplitude of this water-mediated slow component is typically less than, but near about 10% - even when the protein side chain motion is frozen. In the presence of side chain motion, this contribution is much larger – about 20-30%. We surmise that this was the component observed by Zewail and co-workers.^{7,43}

Yet another factor missed in earlier studies but brought out by our decomposition technique is that the ultrafast component in the protein solvation dynamics arises almost entirely from the outer layer of water molecules. This rather paradoxical result however can be rationalized within the molecular

hydrodynamic theory of Chandra and Bagchi^{41,66,67}, as discussed above.

The slow decay that arises only from PHL water molecules agrees well with the log-normal distribution observed in distribution of relaxation times of PHL-water molecules. In a previous work, we reported that the distributions of relaxation times change from Gaussian in the bulk to log-normal in the PHL³⁰. The ubiquitous long tail in these distributions is related to the slow component observed in solvation dynamics.

However, one should bear in mind that there is a considerable heterogeneity across the protein structures (*Supporting Information S2*) which affects solvation dynamics to a greater extent. So no general conclusion is fair to be drawn. However, we have attempted to draw certain general conclusions with the help of time dependent density functional theory. We have suggested that the origin of slow decay mediated by the AASC and water coupled motions can be described in terms of a partial (or, cross) dynamic structure factor between SC and water. The challenge is to precisely calculate the cross-dynamic structure factor between SC and water. This is an interesting quantity to calculate both in simulations and in theory. These cross correlation functions holds the key to the observed slow/fast dynamics.

Thus, although the search for general features has been elusive, we nevertheless know why PHL in lysozyme behave differently from that in myoglobin by studying the structure of the exposed amino acid side chains. We know that

water molecules around charged residues form rigid hydrogen bond structure that slows dynamics by more than one order of magnitude.⁶ The flow chart given in **Figure 9** summarizes the generality present in protein hydration layer, and captured through the present study.

6. SUPPLEMENTARY MATERIALS

We provide Supporting Information to further elaborate, support and to ensure the reproducibility of our results. In **Section S1**, we provide the mutated charges of the neighbourhood of natural probes with proper atomistic pictures of the side-chains. In **Section S2**, we furnish some salient features of the proteins which may affect the dynamics of PHL and in turn affect solvation timescales.

7. ACKNOWLEDGEMENTS

We gratefully acknowledge the partial support by grants from DST, India. BB acknowledges support from Sir J.C Bose fellowship. S. Mondal thanks UGC, India for financial support and fellowship. S. Mukherjee thanks INSPIRE, India for providing fellowship.

Appendix: System and Simulation Details

Atomistic molecular dynamics simulations have been performed using GROMACS (v-5.0.7)⁷². We construct the systems so that it matches the experimental concentration (~2-3 mM). We have used Optimized Parameters for Liquid Simulation-all atom (OPLS-AA) force field⁷³ and extended point charge (SPC/E) water model. Periodic boundary conditions were implemented using cubic boxes of sides 93 Å with 26,338 water molecules for Lysozyme (PDB ID: 1AKI)⁷⁴; 94 Å with 26,236 water molecules for sperm whale myoglobin (PDB ID: 3E5O) and 93 Å with 25,652 water molecules for sweet protein Monellin (PDB ID: 3MON). The total system was energy minimised using steepest descend followed by conjugate gradient method. Then the system is subjected to the simulated annealing⁷⁵ to heat it up from 300K to 320K and again cool it down from 320K to 300K; in order to get the system out of a local minima (if any). The solvent is equilibrated for 10 ns at constant temperature (300 K) and pressure (1 bar) (NPT) by restraining the positions of the protein atoms followed by NPT equilibration for another 10 ns without position restrain. The final production runs are carried out at a constant temperature (T=300 K)

(NVT) for 55 ns. The equations of motions are integrated using leap-frog integrator with an MD time step of 1.0 fs. For analysis, the trajectories were recorded for the last 50 ns with 10 fs resolution. All reported data are averaged over three MD trajectories starting from entirely different configuration of the system.

We have used Nôse-Hoover thermostat⁷⁶ and Parrinello-Rahman barostat⁷⁷ to keep the temperature and pressure constant respectively. The cut-off radius for neighbour searching and non-bonded interactions has been taken to be 10 Å and all the bonds are constrained using the LINCS⁷⁸ algorithm. For the calculation of electrostatic interactions, we have used Particle Mesh Ewald (PME)⁷⁹ with FFT grid spacing of 1.6 Å.

References:

(1) Bagchi, B. *Chem. Rev.* **2005**, *105*, 3197.

(2) Laage, D.; Elsaesser, T.; Hynes, J. T. *Chem. Rev.* **2017**, DOI: 10.1021/acs.chemrev.6b00765.

(3) Bagchi, B. *Proc. Natl. Acad. Sci. U.S.A.* **2016**, *113*, 8355.

(4) Ball, P. *Proc. Natl. Acad. Sci. U.S.A.* **2017**, 201703781.

(5) Frauenfelder, H.; Chen, G.; Berendzen, J.; Fenimore, P. W.; Jansson, H.; McMahon, B. H.; Stroet, I. R.; Swenson, J.; Young, R. D. *Proc. Natl. Acad. Sci. U.S.A.* **2009**, *106*, 5129.

(6) Nandi, N.; Bagchi, B. *J. Phys. Chem. B* **1997**, *101*, 10954.

(7) Pal, S. K.; Peon, J.; Bagchi, B.; Zewail, A. H. *J. Phys. Chem. B* **2002**, *106*, 12376.

(8) Bhattacharyya, K. *Chem. Comm.* **2008**, 2848.

(9) Bhattacharyya, S. M.; Wang, Z.-G.; Zewail, A. H. *J. Phys. Chem. B* **2003**, *107*, 13218.

(10) Pal, S. K.; Zewail, A. H. *Chem. Rev.* **2004**, *104*, 2099.

(11) Peon, J.; Pal, S. K.; Zewail, A. H. *Proc. Natl. Acad. Sci. U.S.A.* **2002**, *99*, 10964.

(12) Zhong, D.; Pal, S. K.; Zewail, A. H. *Chem. Phys. Lett.* **2011**, *503*, 1.

(13) Bagchi, B. *Water in Biological and Chemical Processes: From Structure and Dynamics to Function*; Cambridge University Press, 2013.

(14) Denisov, V. P.; Halle, B. *Faraday Discuss.* **1996**, *103*, 227.

(15) Mondal, S.; Mukherjee, S.; Bagchi, B. *Chem. Phys. Lett.* **2017**, *683*, 29.

(16) Modig, K.; Liepinsh, E.; Otting, G.; Halle, B. *J. Am. Chem. Soc.* **2004**, *126*, 102.

(17) Levy, Y.; Onuchic, J. N. *Annu. Rev. Biophys. Biomol. Struct.* **2006**, *35*, 389.

(18) Ball, P. *CELLULAR AND MOLECULAR BIOLOGY-PARIS-WEGMANN-2001*, *47*, 717.

(19) Pethig, R. *Annu. Rev. Phys. Chem.* **1992**, *43*, 177.

(20) Grant, E. *Bioelectromagnetics* **1982**, *3*, 17.

(21) Mashimo, S.; Kuwabara, S.; Yagihara, S.; Higasi, K. *J. Phys. Chem.* **1987**, *91*, 6337.

(22) Castner Jr, E. W.; Fleming, G. R.; Bagchi, B.; Maroncelli, M. *J. Chem. Phys.* **1988**, *89*, 3519.

(23) Nandi, N.; Roy, S.; Bagchi, B. *J. Chem. Phys.* **1995**, *102*, 1390.

(24) Laage, D.; Stirnemann, G.; Hynes, J. T. *J. Phys. Chem. B* **2009**, *113*, 2428.

(25) Sterpone, F.; Stirnemann, G.; Laage, D. *J. Am. Chem. Soc.* **2012**, *134*, 4116.

(26) Halle, B. *Philos. Trans. R. Soc. London, Ser. B* **2004**, *359*, 1207.

(27) Halle, B.; Nilsson, L. *J. Phys. Chem. B* **2009**, *113*, 8210.

(28) Makarov, V.; Pettitt, B. M.; Feig, M. *Acc. chem. Res.* **2002**, *35*, 376.

(29) Otting, G.; Liepinsh, E.; Wuthrich, K. *Science* **1991**, *254*, 974.

(30) Mukherjee, S.; Mondal, S.; Bagchi, B. *J. Chem. Phys.* **2017**, *147*, 024901.

(31) Ghosh, R.; Banerjee, S.; Hazra, M.; Roy, S.; Bagchi, B. *J. Chem. Phys.* **2014**, *141*, 22D531.

(32) Frank, H. S.; Evans, M. W. *J. Chem. Phys.* **1945**, *13*, 507.

(33) Kauzmann, W. *Advances in protein chemistry* **1959**, *14*, 1.

(34) Wüthrich, K.; Billeter, M.; Güntert, P.; Luginbühl, P.; Riek, R.; Wider, G. *Faraday Discuss.* **1996**, *103*, 245.

(35) Mashimo, S.; Kuwabara, S.; Yagihara, S.; Higasi, K. *J. Chem. Phys.* **1989**, *90*, 3292.

(36) Mattea, C.; Qvist, J.; Halle, B. *Biophysical journal* **2008**, *95*, 2951.

(37) Bagchi, B.; Oxtoby, D. W.; Fleming, G. R. *Chem. Phys.* **1984**, *86*, 257.

(38) Maroncelli, M.; Fleming, G. R. *J. Chem. Phys.* **1988**, *89*, 5044.

(39) Bhattacharyya, K. *Acc. chem. Res.* **2003**, *36*, 95.

(40) Bhattacharyya, K.; Bagchi, B. *J. Phys. Chem. A* **2000**, *104*, 10603.

(41) Bagchi, B.; Chandra, A. *J. Chem. Phys.* **1989**, *90*, 7338.

(42) Li, T.; Hassanali, A. A.; Kao, Y.-T.; Zhong, D.; Singer, S. *J. J. Am. Chem. Soc.* **2007**, *129*, 3376.

(43) Pal, S. K.; Peon, J.; Zewail, A. H. *Proc. Natl. Acad. Sci. U.S.A.* **2002**, *99*, 1763.

(44) Bagchi, B. *Molecular relaxation in liquids*; OUP USA, 2012.

(45) Jordanides, X. J.; Lang, M. J.; Song, X.; Fleming, G. R. *J. Phys. Chem. B* **1999**, *103*, 7995.

(46) de Boeij, W. P.; Pshenichnikov, M. S.; Wiersma, D. A. *Annu. Rev. Phys. Chem.* **1998**, *49*, 99.

(47) Kennis, J. T.; Larsen, D. S.; Ohta, K.; Facciotti, M. T.; Glaeser, R. M.; Fleming, G. R. *J. Phys. Chem. B* **2002**, *106*, 6067.

(48) King, J. T.; Arthur, E. J.; Brooks III, C. L.; Kubarych, K. *J. J. Phys. Chem. B* **2012**, *116*, 5604.

(49) Bagchi, B. *Annu. Rev. Phys. Chem.* **1989**, *40*, 115.

(50) Maroncelli, M. *J. Chem. Phys.* **1991**, *94*, 2084.

(51) Jimenez, R.; Fleming, G. R.; Kumar, P.; Maroncelli, M. *Nature* **1994**, *369*, 471.

(52) Maroncelli, M.; Fleming, G. R. *J. Chem. Phys.* **1987**, *86*, 6221.

(53) Fenimore, P. W.; Frauenfelder, H.; McMahon, B. H.; Parak, F. G. *Proc. Natl. Acad. Sci. U.S.A.* **2002**, *99*, 16047.

(54) Qin, Y.; Wang, L.; Zhong, D. *Proc. Natl. Acad. Sci. U.S.A.* **2016**, *113*, 8424.

(55) Zhang, L.; Wang, L.; Kao, Y.-T.; Qiu, W.; Yang, Y.; Okobiah, O.; Zhong, D. *Proc. Natl. Acad. Sci. U.S.A.* **2007**, *104*, 18461.

(56) Qin, Y.; Jia, M.; Yang, J.; Wang, D.; Wang, L.; Xu, J.; Zhong, D. *J. Phys. Chem. Lett.* **2016**, *7*, 4171.

(57) Nandi, N.; Bhattacharyya, K.; Bagchi, B. *Chem. Rev.* **2000**, *100*, 2013.

(58) Wolynes, P. G. *J. Chem. Phys.* **1987**, *86*, 5133.

(59) Carter, E. A.; Hynes, J. T. *J. Chem. Phys.* **1991**, *94*, 5961.

(60) Laird, B. B.; Thompson, W. H. *J. Chem. Phys.* **2007**, *126*, 211104.

(61) Furse, K.; Corcelli, S. *J. Phys. Chem. Lett.* **2010**, *1*, 1813.

(62) Pal, S.; Maiti, P. K.; Bagchi, B.; Hynes, J. T. *J. Phys. Chem. B* **2006**, *110*, 26396.

(63) Luzar, A.; Chandler, D. *Nature* **1996**, *379*, 55.

(64) Balasubramanian, S.; Pal, S.; Bagchi, B. *Physical review letters* **2002**, *89*, 115505.

(65) Bandyopadhyay, S.; Chakraborty, S.; Bagchi, B. *J. Am. Chem. Soc.* **2005**, *127*, 16660.

(66) Bagchi, B.; Chandra, A. *Advances in chemical physics* **2009**, *80*, 1.

(67) Chandra, A.; Bagchi, B. *J. Chem. Phys.* **1989**, *91*, 1829.

(68) van der Zwan, G.; Hynes, J. T. *J. Chem. Phys.* **1982**, *76*, 2993.

(69) Van der Zwan, G.; Hynes, J. T. *The Journal of Physical Chemistry* **1985**, *89*, 4181.

(70) Qiu, W.; Kao, Y.-T.; Zhang, L.; Yang, Y.; Wang, L.; Stites, W. E.; Zhong, D.; Zewail, A. H. *Proc. Natl. Acad. Sci. U.S.A.* **2006**, *103*, 13979.

(71) Qiu, W.; Zhang, L.; Okobiah, O.; Yang, Y.; Wang, L.; Zhong, D.; Zewail, A. H. *J. Phys. Chem. B* **2006**, *110*, 10540.

(72) Hess, B.; Kutzner, C.; Van Der Spoel, D.; Lindahl, E. *J. Chem. Theo. Comp.* **2008**, *4*, 435.

(73) Jorgensen, W. L.; Tirado-Rives, J. *J. Am. Chem. Soc.* **1988**, *110*, 1657.

(74) Artymiuk, P.; Blake, C.; Rice, D.; Wilson, K. *Acta Crystallographica Section B: Structural Crystallography and Crystal Chemistry* **1982**, *38*, 778.

(75) Kirkpatrick, S.; Gelatt, C. D.; Vecchi, M. P. *science* **1983**, *220*, 671.

(76) Nosé, S. *Mol. Phys.* **1984**, *52*, 255.

(77) Parrinello, M.; Rahman, A. *Physical Review Letters* **1980**, *45*, 1196.

(78) Hess, B.; Bekker, H.; Berendsen, H. J.; Fraaije, J. G. *J. Comput. Chem.* **1997**, *18*, 1463.

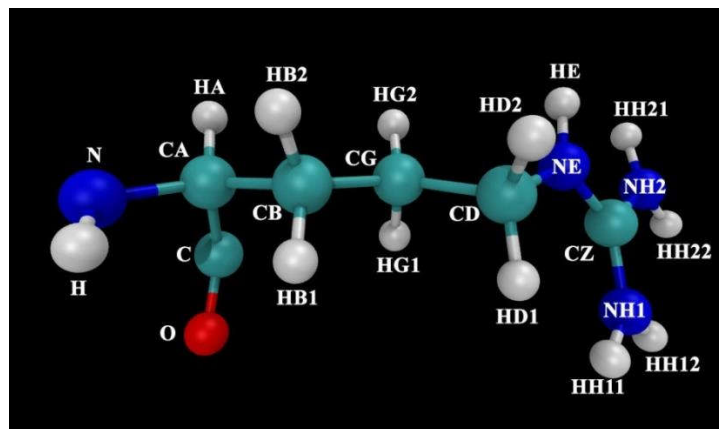
(79) Darden, T.; York, D.; Pedersen, L. *J. Chem. Phys.* **1993**, *98*, 10089.

SUPPLEMENTARY MATERIAL

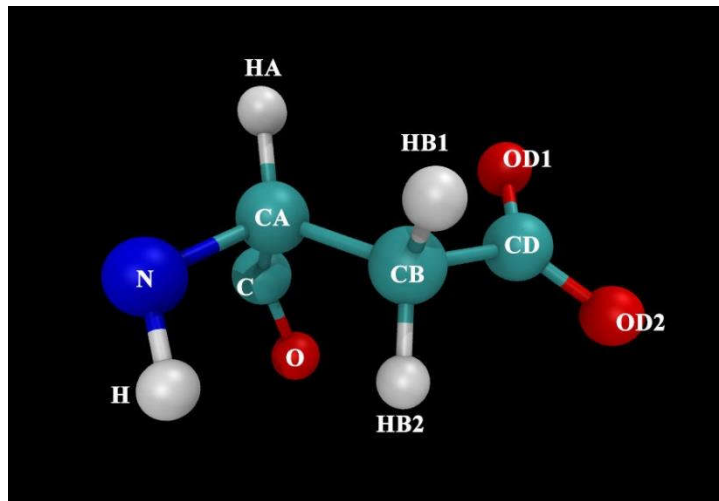
S1. Details of charge mutation:

The charges in the wild type of proteins are acquired from OPLS-AA (Optimized Potential for Liquid Simulation-all atom) force field and those are mutated to provide the probes with a net-non polar environment.

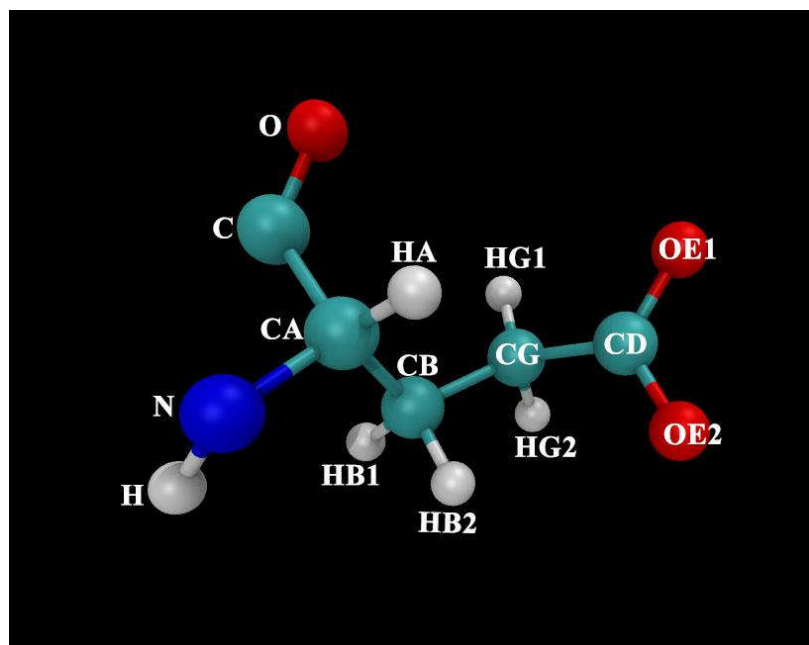
Residue	Atom name	Charges (WT)	Charges (MUT)
Arginine	N	-0.5	-0.5
	H	0.3	0.3
	CA	0.14	0.14
	HA	0.06	0.06
	CB	-0.12	-0.12
	HB1	0.06	0.06
	HB2	0.06	0.06
	CG	-0.05	-0.167
	HG1	0.06	0.02
	HG2	0.06	0.02
	CD	0.19	0.06
	HD1	0.06	0.02
	HD2	0.06	0.02
	NE	-0.7	-0.293
	HE	0.44	0.147
	CZ	0.64	0.213
	NH1	-0.8	-0.326
	HH11	0.46	0.153
	HH12	0.46	0.153
	NH2	-0.8	-0.326
	HH21	0.46	0.153
	HH22	0.46	0.153
	C	0.5	0.5
	O	-0.5	-0.5
Net Charge	---	+1.00	0.00



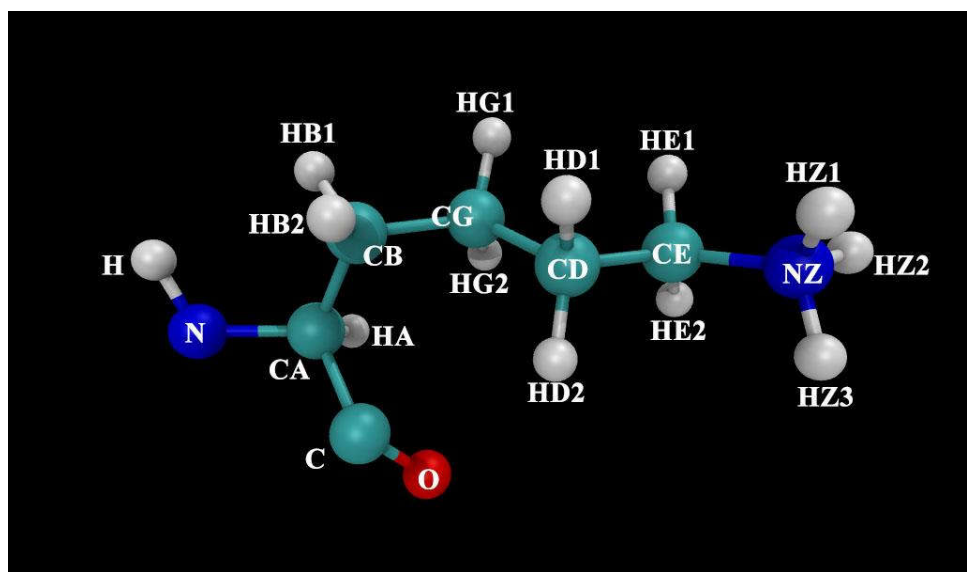
Residue	Atom name	Charges (WT)	Charges (MUT)
Aspartic acid	N	-0.5	-0.5
	H	0.3	0.3
	CA	0.14	0.14
	HA	0.06	0.06
	CB	-0.22	-0.12
	HB1	0.06	0.06
	HB2	0.06	0.06
	CG	0.7	0.4
	OD1	-0.8	-0.2
	OD2	-0.8	-0.2
	C	0.5	0.5
	O	-0.5	-0.5
Net Charge	---	-1.00	0.00



Residue	Atom name	Charges (WT)	Charges (MUT)
Glutamic Acid	N	-0.5	-0.5
	H	0.3	0.3
	CA	0.14	0.14
	HA	0.06	0.06
	CB	-0.12	-0.12
	HB1	0.06	0.06
	HB2	0.06	0.06
	CG	-0.22	-0.12
	HG1	0.06	0.06
	HG2	0.06	0.06
	CD	0.7	0.4
	OE1	-0.8	-0.2
	OE2	-0.8	-0.2
	C	0.5	0.5
	O	-0.5	-0.5
Net Charge	---	-1.00	0.00



Residue	Atom name	Charges (WT)	Charges (MUT)
Lysine	N	-0.5	-0.5
	H	0.3	0.3
	CA	0.14	0.14
	HA	0.06	0.06
	CB	-0.12	-0.12
	HB1	0.06	0.06
	HB2	0.06	0.06
	CG	-0.12	-0.12
	HG1	0.06	0.06
	HG2	0.06	0.06
	CD	-0.12	-0.12
	HD1	0.06	0.01
	HD2	0.06	0.01
	CE	0.19	0.09
	HE1	0.06	0.01
	HE2	0.06	0.01
	NZ	-0.3	-0.10
	HZ1	0.33	0.03
	HZ2	0.33	0.03
	HZ3	0.33	0.03
	C	0.5	0.5
	O	-0.5	-0.5
Net Charge	---	+1.00	0.00



S2. Some Salient features of Lysozyme, Myoglobin and Monellin

We have chosen three different proteins to study the solvation dynamics of natural probe tryptophan. Nevertheless, the proteins are unique in their structural and dynamical properties. This heterogeneity provides a differing environment to the probes, which considerably affects the solvation timescales. Below we point out some of the distinct differences.

- Myoglobin is rich in α -helices. There are no β -sheets present. Lysozyme contains both of the secondary structures with an increased population of α -helices. On the contrary, sweet protein Monellin has a greater population of β -sheets.
- There are eleven positively charged arginine residues present in lysozyme. Arginine and lysine are the one of the most hydrophilic amino acids according to certain hydropathy scales. Moreover, hydrophilic solvent accessible surface area (SASA) is $\sim 60\%$ for lysozyme. This polarises the PHL water molecules more than the other two proteins.
- A measure of the structural fluctuation can be obtained in terms of the root mean square deviation (RMSD) trajectory. The RMSD at time ‘t’, in **Fig. S1**, is calculated by superimposing the structure at times ‘t’ and ‘t-dt’, where ‘dt’ is the data dumping frequency of the MD trajectory. The plot clearly shows that the structural rigidity is quite different for the three protein-water systems. Myoglobin shows the maximum fluctuation. Whereas lysozyme exhibits the least deviation. It tells the increased stability of lysozyme. However, Monellin lies in between.

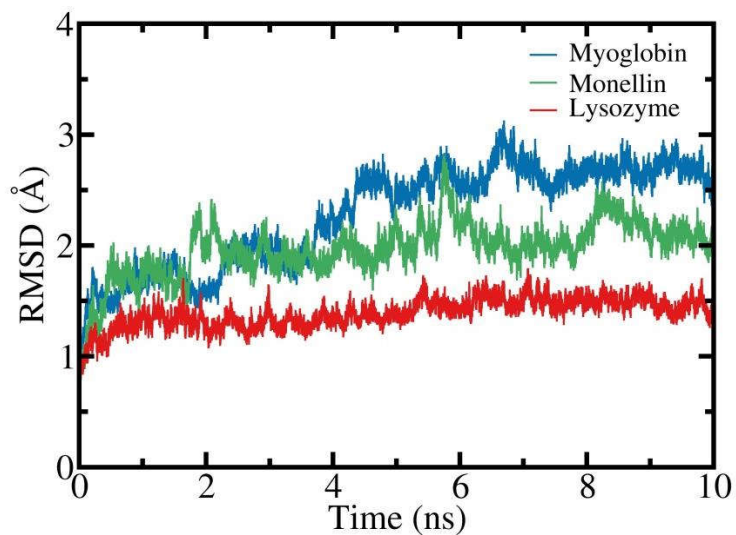


Figure S1. Plot of root mean squared deviation (RMSD) of Myoglobin, Lysozyme and Monellin against time with respect to their structure at the previous MD frame. These plots shows the net dynamic heterogeneity among these structures.